Supplementary Information to

# Light Emission by Free Electrons in Photonic Time-Crystals

**Alex Dikopoltsev[1†], Yonatan Sharabi[1†], Mark Lyubarov[1], Yaakov Lumer[1], Shai Tsesses[2], Eran Lustig[1], Ido Kaminer[2], and Mordechai Segev[1,2]**

[1]Physics Department, Technion – Israel Institute of Technology, Haifa 32000, Israel

[2]Electrical Engineering Department, Technion – Israel Institute of Technology, Haifa 32000, Israel

[†]*These authors contributed equally*

## 1 Comparison: Photonic Time-Crystals (PTCs) and Optical Parametric Amplifiers (OPAs)

When exploring PTCs, we should pinpoint the relation to OPAs, where the macroscopic polarization in a nonlinear medium also varies at ultrafast rates, driven by one (or more) intense waves. The difference between OPA and PTC is profound: the appearance of broad momentum gaps in PTCs, gives rise to exponential amplification of all waves whose wave-vector resides in the gap. In OPAs, phase-matching dictates a resonant condition on the momentum of the interacting waves: the momentum of the pump must be equal to the sum of the momentum of the interaction products (signal and pump). Also, since during the interaction in OPAs energy is conserved, the frequency of the pump must be equal to the sum of the frequencies of the signal and the idler. In PTCs, on the other hand, there is no resonance whatsoever. Instead, PTCs have a sizeable gap in momentum where all waves are amplified (or suppressed). This has impact on all light-matter interactions, for example – all waves with momentum in the gap are amplified, drawing their energies from the modulation.

The immediate implications of this profound difference between OPAs and PTCs are, for example, that pairs of real photons originating from vacuum fluctuations appear in OPAs only at resonance [1], because the gap in OPAs is nonexistent, whereas in PTCs – as we show in the main text and here – appear at all modes associated with the momentum gap, and are exponentially amplified, drawing energy from the modulation.

## 2 EM modes in Photonic Time-Crystals

In this section, we find the eigenmodes of the electromagnetic (EM) wave equation in a Photonic Time Crystal (PTC) using the method presented in [2]. When the permittivity of a medium undergoes periodic changes in time, the refractive index variations induce multiple reflections and refractions of waves in space that interfere to form the Floquet band structure of the EM modes. In the following subsection we derive the dispersion relation and find the eigenmodes of the PTC, both in the bands and in the gaps.

### *1.1 Magnetic field equations for time-varying permittivity*

We start with Maxwell's equations in a spatially-homogeneous medium, non-magnetic and without any sources. For simplicity, we assume here that the medium is isotropic, and put aside all tensorial effects that can arise from the electric permittivity in anisotropic media.

$$\nabla \cdot D = \nabla \cdot \left( \varepsilon(t) E \right) \to \nabla \cdot E = 0; \qquad \nabla \cdot B = 0 \to \nabla \cdot H = 0$$

The equations can be written as

$$\nabla \times E = -\frac{\partial B}{\partial t} = -\mu_0 \frac{\partial H}{\partial t}; \qquad \nabla \times H = \frac{\partial D}{\partial t} = \frac{\partial \left( \varepsilon(t) E \right)}{\partial t},$$

where $\varepsilon = \varepsilon_0 \varepsilon_r \varepsilon_M(t)$. With some algebra we get the following equation of the magnetic field

$$\nabla^2 H = \frac{1}{c^2} \frac{\partial}{\partial t} \left( \varepsilon_M(t) \frac{\partial H}{\partial t} \right). \qquad (1.1.1)$$

Throughout this paper, we choose to work with the magnetic field because its mathematical link to the current source is free of time derivatives (Ampere's law).

### *1.2 Bloch-Floquet analysis*

PTCs form when the permittivity varies periodically in time. Thus, we take $\epsilon_m(t)$ to be periodic in time T, meaning

$$\varepsilon_M(t) = \varepsilon_M(t+T).$$

Since the medium is homogeneous, the wavevector **k** is a conserved quantity appearing as a constant characterizing each eigenmode of the system. For convenience, let us choose the spatial coordinates such that $E, H$ are in the $x, z$ directions, respectively, and the waves propagate in the y direction. The eigenmodes of Eq. (1) are of the form

$$H(y,t) = H_0 \hat{z}\, h_k(t) e^{iky}. \qquad (1.2.1)$$

We are left with

$$-k^2 h_k(t) = \frac{1}{c^2}\frac{\partial}{\partial t}\left(\varepsilon_M(t)\frac{\partial h_k(t)}{\partial t}\right). \qquad (1.2.2)$$

We solve this differential equation using the Bloch-Floquet theorem, resulting in $h_k(t)$ which is time-periodic with periodicity T, up to the Floquet phase $\omega_k t$. The general form is

$$h_k(t) = e^{i\omega_k t}\sum_m q_k^m e^{im\Omega t} \qquad (1.2.3),$$

where $\omega_k$ is the Floquet frequency that depends on the wavenumber k, Ω is the modulation frequency $2\pi/T$, the integer m is the order of the harmonic of the temporal modulation, and $q_{\mathrm{k}}^{\mathrm{m}}$ are the Fourier coefficients of the Floquet mode. Next, we expand the periodic permittivity into its Fourier coefficients

$$\varepsilon_M(t) = \sum_m \varepsilon^m e^{im\Omega t}. \qquad (1.2.4)$$

Using substituting (1.2.3) and (1.2.4) into (1.2.2) we obtain

$$\frac{\partial}{\partial t}\left(\sum_m \varepsilon_m e^{im\Omega t}\frac{\partial\left(e^{-i\omega_k t}\sum_n q_k^n e^{in\Omega t}\right)}{\partial t}\right) + k^2c^2e^{-i\omega_k t}\sum_l q_k^l e^{il\Omega t} = 0, \qquad (1.2.5)$$

where $l$ and $n$ are the indices of the harmonics of the field. With some algebra we find

$$\Rightarrow k^2c^2\sum_l q_k^l e^{il\Omega t} = \sum_{n,m}\left((n+m)\Omega-\omega_k\right)\left(n\Omega-\omega_k\right)\varepsilon_m q_k^n e^{i(n+m)\Omega t}$$

$$\Rightarrow l = n+m \rightarrow m = l-n$$

where we define

$$\gamma_{l,n}(\omega_k) = (\omega_k - l\Omega)(\omega_k - n\Omega).$$

Finally, the relation between the coefficients is

$$\sum_n\left[\gamma_{l,n}(\omega_k)\varepsilon_{l-n} - k^2c^2\delta_{l,n}\right]q_k^n = 0. \qquad (1.2.6)$$

### 1.3 *Specific case of sinusoidal modulation*

In the main text, for the sake of clarity, we present results for a single momentum gap, which is the result of sinusoidal modulation of the permittivity. In this specific case

$$\varepsilon_M = \varepsilon' + 2\varepsilon'' \cos(\Omega t) = \varepsilon' + \varepsilon''\left(e^{i\Omega t} + e^{-i\Omega t}\right) \Rightarrow \varepsilon_0 = \varepsilon'; \varepsilon_{1,-1} = \varepsilon''. \qquad (1.3.1)$$

We substitute this into (1.2.6) and obtain the following infinite set of equations

$$\begin{pmatrix} \ddots & (\omega_k+2\Omega)(\omega_k+\Omega)\varepsilon'' & 0 & \vdots & \iddots \\ (\omega_k+2\Omega)(\omega_k+\Omega)\varepsilon'' & (\omega_k+\Omega)^2\varepsilon' - k^2c^2 & (\omega_k+\Omega)\omega_k\varepsilon'' & 0 & \dots \\ 0 & (\omega_k+\Omega)\omega_k\varepsilon'' & \omega_k^2\varepsilon' - k^2c^2 & (\omega_k-\Omega)\omega_k\varepsilon'' & 0 \\ \dots & 0 & (\omega_k-\Omega)\omega_k\varepsilon'' & (\omega_k-\Omega)^2\varepsilon' - k^2c^2 & (\omega_k-2\Omega)(\omega_k-\Omega)\varepsilon'' \\ \iddots & \vdots & 0 & (\omega_k-2\Omega)(\omega_k-\Omega)\varepsilon'' & \ddots \end{pmatrix} \begin{pmatrix} \vdots \\ q_k^{-1} \\ q_k^{0} \\ q_k^{1} \\ \vdots \end{pmatrix} = 0$$

To a good approximation, the coefficients $q_k^n$ decay as |n| increases , meaning that $\lim_{|n|\to\infty} q_k^n \to 0$. Physically, this means that when a wave propagates in a PTC, it is mostly coupled to the nearest harmonics of the modulation frequency. In this case, we can truncate the relation, assuming a finite vector and matrix, and solve this set of equations numerically. The solution to this matrix provides the coefficients of the dispersion relation of the Floquet-Bloch eigenmodes. The corresponding dispersion relation is presented in Fig. 2a of the main text, in a folded fashion (as customary in spatially-periodic structures). It is, however, instructive to also present the unfolded dispersion relation, as we do here in Fig. S1A. Notice that each band is drawn shifted to the right by a period of Ω from the band below it, while defining a new parameter $\omega_{k,c} = \omega_{k,l} + l\Omega$, where $l$ is the number of the band. This is to compare the PTC dispersion to the ideal light cone and highlight the influence of the modulation on the momentum-gap. The Fourier components amplitudes of the Floquet eigenmodes are shown in Fig. S1B. Exactly at the band edge bordering the gap, the two main components of the eigenmode possess the frequencies $\pm\frac{\Omega}{2}$. At higher central frequencies $\omega_{k,c}$, the Fourier components of the higher harmonics ($m \neq 0$) become significant.

### 1.4 *Modal Amplitudes*

The solutions to (1.2.6) with k wavenumbers residing in the bands differ from the ones in the bandgap. In the bands, $\omega_k$ is a real number which mean that the solution (Floquet mode) is oscillating periodically. In the bandgaps, $\omega_k = i\gamma_k + \beta_k$ is complex. The real part, $\beta_k$, determines the phase accumulation of the mode, and its imaginary part, $\gamma_k$, determines the exponential decay or growth of the mode amplitude. Moreover, each k has two solutions, which must be orthogonal. In the bands, these two solutions are complex conjugates of each other, meaning that $h_{k,-} = h_{k,+}^*$, and are orthogonal over a full cycle T. Each mode is normalized by

$$\frac{1}{T}\int_0^T h_{k,\sigma} h_{k,\sigma}^* dt = \frac{1}{T}\int_0^T \left|h_{k,\sigma}\right|^2 dt = 1 \qquad (1.4.1)$$

In the bandgap, due to the complex values of $\omega_k$, the modes have the following form:

$$h_{k,+}(t) = e^{i\beta_k t + \gamma_k t} \Sigma q_k^m e^{im\Omega t}; \; h_{k,-}(t) = e^{-i\beta_k t - \gamma_k t} \Sigma \left(q_k^m\right)^* e^{-im\Omega t}. \qquad (1.4.2)$$

## 3 Green's function for a time-varying current source embedded in a PTC

In this section, we find the Magnetic field emitted by current source in a PTC. To do this, we use the magnetic field wave equation with a current source $\vec{J}(r,t)$:

$$\left(\partial_t\left(\varepsilon_M\partial_t\right)-c^2\nabla^2\right)\vec{H}=\vec{\nabla}\times\vec{j}\,. \quad (2.1)$$

We use the fact the we found the solutions to the source-less equation (1.1.1) which are orthogonal in k space, decompose the current vector into its spatial frequencies $\vec{j}_k$, and then recast (2.1) as

$$\left(\partial_t\left(\varepsilon_M\partial_t\right)+c^2k^2\right)\vec{H}_k=-i\vec{k}\times\vec{j}_k\,, \quad (2.2)$$

where c is the speed of light in the medium. Our solution strategy is to find a Green function which satisfies the time-dependent part

$$\left(\partial_t\left(\varepsilon_M\partial_t\right)+c^2k^2\right)G_k\left(t,t'\right)=\delta\left(t-t'\right), \quad (2.3)$$

which, when integrated over the current source would yield the magnetic field component at the specific $k$

$$\vec{H}_k\left(t\right)=-i\int\vec{G}_k\left(t,t'\right)\left[k\times\vec{j}_k\left(t'\right)\right]dt'\,. \quad (2.4)$$

We find a general Green function of the following form

$$G_k\left(t,t'\right)=\begin{cases}Q_{k,+}\left(t'\right)h_{k,+}\left(t\right)+Q_{k,-}\left(t'\right)h_{k,-}\left(t\right) & t<t'\\ 0 & t\geq t'\end{cases}, \quad (2.5)$$

where $Q_{k,+}$ and $Q_{k,-}$ are general time-dependent functions, and $h_{k,+}$ and $h_{k,-}$ and the Floquet solutions we found earlier in (1.4). From the continuity of the Green function we require

$$G_k\left(t',t'\right)=Q_{k,+}\left(t'\right)h_{k,+}\left(t'\right)+Q_{k,-}\left(t'\right)h_{k,-}\left(t'\right)=0\,,$$

so that

$$G_k\left(t,t'\right)=\begin{cases}Q_{k,1}\left(t'\right)\left[h_{k,+}\left(t\right)-\dfrac{h_{k,+}\left(t'\right)}{h_{k,-}\left(t'\right)}h_{k,-}\left(t\right)\right] & t>t'\\ 0 & t\leq t'\end{cases}. \quad (2.6)$$

Next, we use the definition of the Green function, and integrate over (2.3) to get

$$\partial_tG_k\left(t,t'\right)\big|_{t=t'}=\frac{1}{\varepsilon\left(t'\right)}, \quad (2.7)$$

The time derivative of (2.6) at time $t=t'$ is

$$\partial_tG_k\left(t,t'\right)\big|_{t=t'}=Q_{k,1}\left(t'\right)\left[\dot{h}_{k,+}\left(t'\right)-\frac{h_{k,+}\left(t'\right)}{h_{k,-}\left(t'\right)}\dot{h}_{k,-}\left(t'\right)\right]\frac{1}{2}, \quad (2.8)$$

where we used $\Theta\left(0\right)=1/2$. We substitute (2.7) and (2.8) into (2.6) and find

$$G_k\left(t,t'\right)=\begin{cases}\dfrac{2\left[h_{k,+}\left(t\right)h_{k,-}\left(t'\right)-h_{k,-}\left(t\right)h_{k,+}\left(t'\right)\right]}{\varepsilon\left(t'\right)\left[\dot{h}_{k,+}\left(t'\right)h_{k,-}\left(t'\right)-h_{k,+}\left(t'\right)\dot{h}_{k,-}\left(t'\right)\right]} & t>t'\\ 0 & t\leq t'\end{cases}. \quad (2.9)$$

One can easily show that the denominator is constant over time.

Next, we define $C_k \equiv \varepsilon(t)\left[\dot{h}_{k,+}(t)h_{k,-}(t) - h_{k,+}(t)\dot{h}_{k,-}(t)\right]/2$, and write the final form of the Green function

$$G_k(t,t') = \begin{cases} \dfrac{\left[h_{k,+}(t)h_{k,-}(t') - h_{k,-}(t)h_{k,+}(t')\right]}{C_k} & t > t' \\ 0 & t \le t' \end{cases}. \qquad (2.11)$$

In the bands, the two solutions are complex conjugates ($h_k = h_{k,+} = h^*_{k,-}$), and the Green function takes the form

$$G_k(t,t') = \begin{cases} \dfrac{2i\,\mathrm{Im}\left[h_k^*(t')h_k(t)\right]}{C_k} & t > t' \\ 0 & t \le t' \end{cases}. \qquad (2.12)$$

We notice that $C_k$ is proportional to the overall Minkowski momentum $P_{Min} = D \times B$ [3], which is in line with the fact that the Minkowski Momentum is a conserved quantity in a homogenous time-varying medium. We derive this result here:

$$\frac{\partial P_{Min}}{\partial t} = \frac{\partial D}{\partial t} \times B + D \times \frac{\partial B}{\partial t} = -B \times (\nabla \times H) - D \times (\nabla \times E) = -\mu H \times (\nabla \times H) - \varepsilon E \times (\nabla \times E). \quad (2.13)$$

Then, we use $A \times (\nabla \times A) = \frac{1}{2}\nabla(A \cdot A) - (A \cdot \nabla)A$ and get that

$$\frac{\partial P_{Min}}{\partial t} = -\left[\mu\left(\frac{1}{2}\nabla(H \cdot H) - (H \cdot \nabla)H\right) + \varepsilon\left(\frac{1}{2}\nabla(E \cdot E) - (E \cdot \nabla)E\right)\right] = \vec{\nabla} \cdot \overleftrightarrow{\sigma}. \qquad (2.14)$$

And the result of integration over the entire space is

$$\int dV \frac{\partial P_{Min}}{\partial t} = \int dV \vec{\nabla} \cdot \overleftrightarrow{\sigma} = 0 \left( = \frac{\partial}{\partial t}\left(\int dV P_{Min}\right)\right), \qquad (2.15)$$

meaning that the total Minkowski momentum of the EM wave in a PTC is a conserved quantity.

## 4 Classical derivation of free-electron radiation in a PTC

In this section, we derive the EM radiation emitted from a free-electron in a PTC. To model the electron classically, we assume it is a point-charge moving in the z-direction, with velocity $v = \beta c_0$. The point charge is described as a point source of electric current $\vec{j}_e = \delta(r_\perp)\delta(z - \beta c_0 t)\hat{z}$, where $c_0$ is the speed of light in the vacuum and $r_\perp$ are the coordinates transverse to $z$. The current source can be decomposed into its spatial wavenumbers $\vec{j}_{\boldsymbol{k}} = j_0 e^{ik_z \beta c_0 t}\hat{z}$. We use (2.4) to find the resulting magnetic field, for example pointing in the $y$-direction

$$H_{k,y} = -i\int G_k(t,t')e^{ik_z vt'}k_x dt' = -i\int_{-\infty}^{t} \frac{\left[h_{k,+}(t)h_{k,-}(t') - h_{k,-}(t)h_{k,+}(t')\right]}{C_k} e^{ik_z vt'}k_x dt'.$$

For a current source that starts at t=0 we get

$$H_{k,y}(t) = -i\frac{k_x}{C_k}\left[h_{k,+}(t)\sum_m q_k^{m*}\int_0^t e^{i(k_z v-\omega_k-m\Omega)t'}dt' - h_{k,-}(t)\sum_m q_k^{m}\int_0^t e^{i(k_z v+\omega_k+m\Omega)t'}dt'\right]. \quad (3.1)$$

We find that the efficiency of the emission by the electron at $t \to \infty$ is determined by matching the evolution of its phase $k_z \beta c_0 t$ to the evolution of the phase of the Floquet modes $h_k(t)$, a necessary requirement for efficient light-matter interaction. Maximum efficiency occurs when the phases match ("phase-matching"), that is, when $k_z \beta c = \omega_k + m\Omega$, which occurs for every wavenumber $\vec{k}$ and harmonic number $m$ separately. To find the exact angles and spatial wavenumbers to which the electron radiates, we map the phase-matching condition onto the wavevector space $(k_z, k_\perp)$ of the EM waves in a PTC. We define $n_{eff}(k) \equiv \frac{kc_0}{\omega_k}$, so that

$$k_z v = \frac{kc_0}{n_{eff}(k)} + m\Omega = \frac{\sqrt{{k_z}^2 + {k_\perp}^2}c_0}{n_{eff}(k)} + m\Omega.$$

Then, by defining $\left(k_{\mathrm{mod}} = \Omega n_{eff} / c_0\right)$, we get

$$k_\perp = \sqrt{{k_z}^2\left({n_{eff}}^2(k)\beta^2 - 1\right) - 2mk_z\beta n_{eff}(k)k_{\mathrm{mod}} + m^2{k_{\mathrm{mod}}}^2}. \quad (3.2)$$

This kind of mapping is natural because the wavevector $\vec{k}$ is a conserved quantity in our system and it is unique to each mode. We show this mapping in Figs. 2(c) and 2(e) in the main text.

Henceforth, we consider only the radiation emitted when the phase-matching condition is fulfilled. To gain insight, we divide the radiation solutions into k wavenumbers in the PTC bands and in the PTC bandgaps. For k wavenumbers in the bands where $\omega_k$ is real, we obtain

$$H_{k,y}(t) \approx -i\frac{k_x h_k(t) q_k^{m*} t}{C_k}, \quad (3.3)$$

and a similar result is obtained for $H_{k,x}$. We notice that the amplitude of the field grows linearly with time and is proportional to the m$^{\mathrm{th}}$ Fourier component of the relevant Floquet mode.

However, for $k$-wavenumbers in the bandgaps - where $i\omega_k = i\beta_k + \gamma_k$ and $\gamma_k \neq 0$ - we define the phase-mismatch $\Delta\beta_{\pm,n} = \mathrm{Re}\left\{k_z v \pm \left(\omega_k + m\Omega\right)\right\}$ and find that

$$H_{k,y}(t) = -i\frac{k_x}{C_k}\left[e^{i\beta t}e^{\gamma t}\sum_n q_k^n e^{in\Omega t}\sum_m q_k^{m*}\frac{-1}{i\Delta\beta_{m,-}-\gamma} - e^{-i\beta t}\sum_n q_k^{n*}e^{-in\Omega t}\sum_m q_k^m\frac{e^{i\Delta\beta n_{m,+}t}}{i\Delta\beta_{m,+}+\gamma}\right], \quad (3.4)$$

where we used

$$\int_0^t e^{i\omega t'}dt' = \frac{e^{i\beta t}e^{\gamma t}-1}{i\beta+\gamma}\xrightarrow[t\to\infty]{}\begin{cases}\dfrac{e^{i\beta t}}{i\beta+\gamma}e^{\gamma t} & \gamma>0\\ \dfrac{-1}{i\beta+\gamma} & \gamma<0\end{cases}.$$

In the limit of $t \to \infty$ and treating the second part as a relatively small modulation, we get

$$\lim_{t\to\infty} H_{k,y}(t) = \frac{k_x}{C_k}h_{k,+}(t)\left[\sum_m \frac{q_k^{m*}}{\Delta\beta_{m,-}+i\gamma}\right] = \frac{k_x}{C_k}\zeta_k h_{k,+}(t), \quad (3.5)$$

This result shows that any current source with phase-matched k wavenumber in the gap leads to an exponentially growing EM field. The strongest exponential enhancement $\zeta_k$ is for $\Delta\beta_{m,-} \approx 0$, and for the largest $|q_k^m|$. Typically, $|q_k^0|$ is the largest, and is also exactly the ordinary Cherenkov radiation harmonic, but note that the k value must be in the bandgap for the radiation to be exponentially growing.

## 5 FDTD simulations

Some of the results presented in the main text were extracted from Finite Difference Time Domain (FDTD) simulations. This simulation method solves the Maxwell equations numerically by discretizing both time and space, and then taking small steps in time ($dt$), thus solving the dynamics of the waves. The FDTD algorithm we use is based on the classic FDTD algorithm but contains a few alterations in order to also support the effects of time variations on the EM waves, first suggested in [4]. These alterations enable the simulation to correctly describe time-reflection and refraction and therefore also PTCs. The simulations were carried out in a 2D settings, and the electron was described by a moving current element with a small Gaussian envelope (order of ~0.1 [um]).

The 2D images displaying the plane wave content of the EM waves were calculated by performing a 2D spatial Fourier transform on the EM fields in the simulation. This 2D transform effectively converts the EM waves from a space-based presentation ($E_{x,z}$), to a 2D spatial wavenumber presentation ($E(k_x, k_z)$). This conversion is very useful since each such spatial wavenumber is a pure plane wave and an eigenmode of free space. The magnitude of |k| (wave momentum) can be easily calculated, $|k| = \sqrt{k_x^2 + k_z^2}$, and from it the wave frequency is also found: $\omega = kn/c$. Another way to think about these Fourier transform images is that for each point, the radius (L2 distance from (0,0)) describes the size of the wavenumber $k$ (or proportionally $\omega$), while the angle (theta, calculated from the positive x axis) describes the propagation direction of the plane wave. In carrying out these FDTD simulations, we had to overcome the problem that the waves in the simulation are real and therefore the absolute value of the Fourier transform is symmetric around (0,0). This mean that, regardless of the propagation direction of the wave, the Fourier transform always displays components in both the actual propagation direction and its counter-direction, that is, both $(k_x, k_z)$ and $(-k_x, -k_z)$. This result is of course undesirable as we want to display only the actual propagation components without their negative counterparts, or in other words – if we want to extract the directionality of the waves.

We overcome this problem by performing two Fourier transform calculations, at times $T$ and $T - dt$. We then subtract them from one another, but multiplied by the phase that the forward directional plane wave would accumulate: $F(T) - F(T - dt) \cdot \exp(i \cdot dt \cdot \omega)$. This effectively creates constructive interference for the forward propagating wave and destructive interference for the backwards propagating wave. The outcome is a Fourier transform displaying only the forward propagating components – the real direction of the waves in the system. Figure. S2 shows FDTD simulations of free electron propagation below ($\beta = 0.6$) and above ($\beta = 0.9$) the Cherenkov limit. We used $\epsilon_r = \mathbf{2} + 0.1\sin(\Omega t)$ and $\Omega = 10^{15}\frac{rad}{s}$.

## 6 Quantum derivation

### *1.1 Evolution in time via the Schrödinger equation*

The dynamics in our system, which includes a moving electron and a medium with permittivity that changes periodically in time, is governed by the Schrödinger equation

$$i\hbar\frac{d}{dt}\left|\psi(t)\right\rangle = H(t)\left|\psi(t)\right\rangle. \qquad (5.1.1)$$

The general light-matter Hamiltonian is given by

$$\begin{aligned} H_{tot} &= H_{EM} + H_e \\ H_e &= \frac{1}{2m}\left(\hat{P} - eA\right)^2 = E_e - \frac{e}{m}\hat{P}\cdot\hat{A} + O\left(A^2\right) \approx E_e + H_{\text{int}} \end{aligned}. \qquad (5.1.2)$$

### *1.2 The EM Hamiltonian of EM radiation in a time-varying medium*

Here, we provide the full derivation of the Hamiltonian describing the EM radiation in a time-varying medium. We start (section i) from the classical Lagrangian of the system and then write the Hamiltonian of the PTC in a harmonic oscillator form. In (ii) we quantize the harmonic oscillator operators and derive the Hamiltonian in the form of creation and annihilation operators.

**i. Classical derivation**

We start from the Lagrangian

$$L = \frac{\varepsilon_0}{2}\int d^3r\left(\varepsilon(t)\vec{E}^2 - c^2\vec{B}^2\right) = \frac{\varepsilon_0}{2}\int d^3r\left(\varepsilon(t)\left(\partial_t\vec{A}\right)^2 - c^2\left(\nabla\times\vec{A}\right)^2\right). \qquad (5.2.1)$$

The E.L. equations can easily be shown to give the proper wave equation

$$\begin{aligned} &\frac{\partial}{\partial t}\frac{\partial L}{\partial \dot{A}_n} + \sum\frac{\partial}{\partial x_m}\frac{\partial L}{\partial_{x_m}A_n} = 0 \\ &\partial_t\left(\varepsilon(t)\partial_t\vec{A}\right) - c^2\nabla^2\vec{A} = 0 \end{aligned}.$$

The canonical conjugate variable is

$$\vec{\Pi}_A = \frac{\partial L}{\partial\left(\partial_t\vec{A}\right)} = \varepsilon_0\varepsilon(t)\partial_t\vec{A} = -\varepsilon_0\varepsilon(t)\vec{E} = -\vec{D}(t),$$

and the resulting Hamiltonian of a PTC is

$$\begin{aligned} H &= \int d^3r\vec{\Pi}_A\cdot\vec{A} - L = \frac{\varepsilon_0}{2}\int d^3r\left(\varepsilon(t)\left(\partial_t\vec{A}\right)^2 + c^2\left(\nabla\times\vec{A}\right)^2\right) \\ &= \frac{\varepsilon_0}{2}\int d^3r\left(\frac{1}{{\varepsilon_0}^2\varepsilon(t)}\left(\vec{\Pi}_A\right)^2 + c^2\left(\nabla\times\vec{A}\right)^2\right) \end{aligned}. \qquad (5.2.2)$$

We work in the Coulomb gauge which means that $\vec{\nabla}\cdot\vec{A} = 0$ and $\vec{\nabla}\cdot\overrightarrow{\Pi_A} = 0$.
The equations of motion are

$$\partial_t \vec{A} = \frac{\delta H}{\delta \vec{\Pi}_A} = \frac{1}{\varepsilon_o \varepsilon(t)} \vec{\Pi}_A$$
$$\partial_t \vec{\Pi}_A = -\frac{\delta H}{\delta \vec{A}} = \varepsilon_0 c^2 \nabla^2 \vec{A}$$

The equation of motion for A is easily shown to be what we expect. We write the equation of motion for $\Pi_A$ and get

$$\partial_t{}^2 \vec{\Pi}_A = \varepsilon_0 c^2 \nabla^2 \partial_t \vec{A} = \varepsilon_0 c^2 \nabla^2 \frac{1}{\varepsilon_o \varepsilon(t)} \vec{\Pi}_A = c^2 \frac{1}{\varepsilon(t)} \nabla^2 \vec{\Pi}_A \quad . \qquad (5.2.3)$$
$$\varepsilon(t) \partial_t{}^2 \vec{\Pi}_A - c^2 \nabla^2 \vec{\Pi}_A = 0$$

**ii. Quantization**

We will now upgrade $\vec{A}(r)$ and $\vec{\Pi}(r)$ to quantum operators $\hat{A}(r)$ and $\hat{\Pi}(r)$

$$H = \frac{\varepsilon_0}{2} \int d^3 r \left( \frac{1}{\varepsilon_0{}^2 \varepsilon(t)} \left( \hat{\Pi}_A \right)^2 + c^2 \left( \nabla \times \hat{A} \right)^2 \right). \qquad (5.2.4)$$

Canonical quantization dictates that

$$\left[ \hat{A}_i(r), \hat{\Pi}_{A,j}(r') \right] = i\hbar \delta_{Tij}(r - r')$$
$$\left[ \hat{A}_i(r), \hat{A}_j(r') \right] = \left[ \hat{\Pi}_{A,i}(r), \hat{\Pi}_{A,j}(r') \right] = 0$$

The equations of motion are (after lengthy but straightforward algebra):

$$\partial_t \hat{A} = \frac{1}{i\hbar} \left[ \hat{A}, H \right] = \frac{1}{\varepsilon_0 \varepsilon(t)} \hat{\Pi}_A$$
$$\partial_t \hat{\Pi}_A = \frac{1}{i\hbar} \left[ \hat{\Pi}_A, H \right] = \varepsilon_0 c^2 \nabla^2 \hat{A} \quad , \qquad (5.2.5)$$

which are the equations we expect. We separate variables and write $\hat{A}$ in the following form

$$\hat{A}(r,t) = \frac{1}{\sqrt{\varepsilon_0}} \sum_\lambda c_\lambda \vec{A}_\lambda(r) \hat{q}_\lambda(t),$$

where the equations of motion are

$$\nabla^2 \vec{A}_\lambda(r) = -k^2 \vec{A}_\lambda(r)$$
$$\partial_t \left( \varepsilon(t) \partial_t \hat{q}_\lambda \right) + c^2 k^2 \hat{q}_\lambda = 0 \quad . \qquad (5.2.6)$$

Using reality and orthogonality considerations, we solve the spatial equation and write the modes properly as plane waves and their polarization vectors

$$\begin{aligned}\vec{A}_\lambda(r) &= \vec{A}_{k\sigma}(r) = \frac{1}{\sqrt{V}}\hat{u}_{k\sigma}e^{-i\vec{k}\vec{r}} \\ \hat{A}(r) &= \frac{1}{\sqrt{\varepsilon_0}}\frac{1}{\sqrt{V}}\sum_{k,\sigma}\hat{u}_{k\sigma}e^{-i\vec{k}\vec{r}}\hat{q}_{k\sigma}\end{aligned} . \qquad (5.2.7)$$

We assume the polarization vectors are complex (circular polarization). This assumption is not restrictive. Calculating the orthogonality of these function leads to

$$\int d^3r\vec{A}_{k\sigma}(r)\vec{A}_{k'\sigma'}{}^*(r) = \frac{1}{V}\int d^3r\hat{u}_{k\sigma}\hat{u}_{k'\sigma'}{}^*e^{-i\vec{k}\vec{r}}e^{i\vec{k}'\vec{r}} = \hat{u}_{k\sigma}\hat{u}_{k'\sigma'}{}^*\delta\left(\vec{k}-\vec{k}'\right) = \delta_{\sigma,\sigma'}\delta\left(\vec{k}-\vec{k}'\right).$$

We also calculate the following product

$$\int d^3r\vec{A}_{k\sigma}(r)\vec{A}_{k'\sigma'}(r) = \frac{1}{V}\int d^3r\hat{u}_{k\sigma}\hat{u}_{k'\sigma'}e^{-i\vec{k}\vec{r}}e^{-i\vec{k}'\vec{r}} = \hat{u}_{k\sigma}\hat{u}_{k'\sigma'}\delta\left(\vec{k}+\vec{k}'\right) = \delta_{\sigma,\sigma'}\delta\left(\vec{k}+\vec{k}'\right).$$

We know that

$$\frac{1}{V}\sum_{k,\sigma}\hat{u}_{k\sigma}\hat{u}_{k\sigma}{}^*e^{-i\left(\vec{k}-\vec{k}'\right)\vec{r}} = \delta_{Tij}\left(\vec{r}-\vec{r}'\right),$$

and require the Hermiticity of the vector potential

$$\frac{1}{\sqrt{\varepsilon_0}}\frac{1}{\sqrt{V}}\sum_{k,\sigma}\hat{u}_{k\sigma}e^{-i\vec{k}\vec{r}}\hat{q}_{k\sigma} = \hat{A}(r) = \hat{A}^\dagger(r) = \frac{1}{\sqrt{\varepsilon_0}}\frac{1}{\sqrt{V}}\sum_{k,\sigma}\hat{u}_{k\sigma}{}^*e^{i\vec{k}\vec{r}}\hat{q}_{k\sigma}{}^\dagger . \qquad (5.2.8)$$

We then multiply by $\frac{1}{\sqrt{V}}\hat{u}_{k,\sigma}e^{-i\vec{k}\vec{r}}$ and integrate

$$\int d^3r\frac{1}{\sqrt{\varepsilon_0}}\frac{1}{\sqrt{V}}\sum_{k,\sigma}\hat{u}_{k\sigma}e^{-i\vec{k}\vec{r}}\hat{q}_{k\sigma}\frac{1}{\sqrt{V}}\hat{u}_{k'\sigma'}e^{-i\vec{k}'\vec{r}} = \int d^3r\frac{1}{\sqrt{\varepsilon_0}}\frac{1}{\sqrt{V}}\sum_{k,\sigma}\hat{u}_{k\sigma}{}^*e^{i\vec{k}\vec{r}}\hat{q}_{k\sigma}{}^\dagger\frac{1}{\sqrt{V}}\hat{u}_{k'\sigma'}e^{-i\vec{k}'\vec{r}},$$

$$\Rightarrow \hat{q}_{k'\sigma'}{}^\dagger = \hat{q}_{-k'\sigma'}$$

and similarly for the conjugate field

$$\hat{\Pi}_A(r) = \frac{\sqrt{\varepsilon_0}}{\sqrt{V}}\sum_{k,\sigma}\hat{u}_{k,\sigma}^*e^{i\vec{k}\vec{r}}\hat{p}_{k\sigma} \Rightarrow \hat{p}_{k\sigma}^\dagger = \hat{p}_{-k\sigma}.$$

We also require the following commutation relations

$$\left[\hat{A}_i(r),\hat{\Pi}_{A,j}(r')\right] = i\hbar\delta_{Tij}(r-r').$$

By substituting 5.2.7 into the above we obtain

$$\hat{A}(r)=\frac{1}{\sqrt{\varepsilon_0}}\frac{1}{\sqrt{V}}\sum_{k,\sigma}\hat{u}_{k\sigma}e^{-i\vec{k}\vec{r}}\hat{q}_{k\sigma}$$

$$\left[\hat{A}_i(r),\hat{\Pi}_{A,j}(r')\right]=\frac{1}{V}\left[\sum_{k,\sigma}\hat{u}_{k\sigma}e^{-i\vec{k}\vec{r}}\hat{q}_{k\sigma},\sum_{k',\sigma'}\hat{u}^*_{k',\sigma'}e^{i\vec{k}'\vec{r}'}\hat{p}_{k'\sigma'}\right]. \qquad (5.2.9)$$

$$=\frac{1}{V}\sum_{k,\sigma}\sum_{k',\sigma'}\hat{u}_{k\sigma}\hat{u}^*_{k',\sigma'}e^{i\vec{k}'\vec{r}'}e^{-i\vec{k}\vec{r}}\left[\hat{q}_{k\sigma},\hat{p}_{k'\sigma'}\right]$$

In order to proceed we must assume

$$\left[\hat{q}_{k\sigma},\hat{p}_{k'\sigma'}\right]=i\hbar\delta_{\sigma,\sigma'}\delta\left(\vec{k}-\vec{k}'\right)$$

$$\left[q^\dagger,p^\dagger\right]=q^\dagger p^\dagger-p^\dagger q^\dagger=\left(pq-qp\right)^\dagger=-\left[q,p\right]^\dagger=i\hbar\delta_{\sigma,\sigma'}\delta\left(\vec{k}-\vec{k}'\right).$$

Then, we get

$$\left[\hat{A}_i(r),\hat{\Pi}_{A,j}(r')\right]=i\hbar\frac{1}{V}\sum_{k,\sigma}\hat{u}_{k\sigma}\hat{u}^*_{k',\sigma}e^{i\vec{k}(\vec{r}-\vec{r}')}=i\hbar\delta_{Tij}\left(\vec{r}-\vec{r}'\right),$$

as expected. Similarly, we get $\left[\hat{A}_i(r),\hat{A}_j(r')\right]=\left[\hat{\Pi}_{A,i}(r),\hat{\Pi}_{A,j}(r')\right]=0$ when we assume $\left[\hat{q}_{k\sigma},\hat{q}_{k'\sigma'}\right]=\left[\hat{p}_{k\sigma},\hat{p}_{k'\sigma'}\right]=0$.

Next we derive the Hamiltonian in modal form. We remember

$$H=\frac{\varepsilon_0}{2}\int d^3r\left(\frac{1}{{\varepsilon_0}^2\varepsilon(t)}\left(\vec{\Pi}_A\right)^2+c^2\left(\nabla\times A\right)^2\right). \qquad (5.2.10)$$

One can show using some tedious algebra that

$$\frac{\varepsilon_0}{2}\int d^3r\frac{1}{{\varepsilon_0}^2\varepsilon(t)}\left(\vec{\Pi}_A\right)^2=\frac{1}{2}\sum_{k,\sigma}\frac{1}{\varepsilon(t)}\hat{p}_{k\sigma}{\hat{p}_{k\sigma}}^\dagger$$

$$\frac{\varepsilon_0}{2}\int d^3rc^2\left(\nabla\times A\right)^2=\frac{1}{2}\sum_{k,\sigma}c^2k^2\hat{q}_{k\sigma}{\hat{q}_{k\sigma}}^\dagger$$

,

and overall

$$H=\frac{1}{2}\sum_{k,\sigma}\left(\frac{1}{\varepsilon(t)}\hat{p}_{k\sigma}{\hat{p}_{k\sigma}}^\dagger+c^2k^2\hat{q}_{k\sigma}{\hat{q}_{k\sigma}}^\dagger\right), \qquad (5.2.11)$$

as expected. We remember, that here $\hat{q}_{k\sigma}$ and $\hat{p}_{k\sigma}$ are not necessarily Hermitian operators. The equations of motion are:

$$\partial_t \hat{q}_{k\sigma} = \frac{1}{i\hbar}[\hat{q}_{k\sigma}, H] = \frac{1}{\varepsilon(t)}\hat{p}_{k\sigma}{}^{\dagger}$$

$$\partial_t \hat{p}_{k\sigma} = \frac{1}{i\hbar}[\hat{p}_{k\sigma}, H] = -c^2k^2\hat{q}_{k\sigma}{}^{\dagger}$$

$$\rightarrow \partial_t\left(\varepsilon(t)\partial_t \hat{q}_{k\sigma}\right) = -c^2k^2\hat{q}_{k\sigma}{}^{\dagger}$$

We obtained the equations we expected, and we can now define the annihilation and creation operators

$$\hat{a}_{k\sigma} = \sqrt{\frac{ck}{2\hbar}}\hat{q}_{k\sigma} + i\sqrt{\frac{1}{2\hbar ck}}\hat{p}_{-k\sigma}; \qquad (5.2.12)$$

therefore

$$\hat{a}_{k\sigma}{}^{\dagger} = \sqrt{\frac{ck}{2\hbar}}\hat{q}_{k\sigma}{}^{\dagger} - i\sqrt{\frac{1}{2\hbar ck}}\hat{p}_{-k\sigma}{}^{\dagger} = \sqrt{\frac{ck}{2\hbar}}\hat{q}_{-k\sigma} - i\sqrt{\frac{1}{2\hbar ck}}\hat{p}_{k\sigma}.$$

The inverse relations are

$$\hat{q}_{k\sigma} = \sqrt{\frac{\hbar}{2ck}}\left(\hat{a}_{k\sigma} + \hat{a}_{-k\sigma}{}^{\dagger}\right)$$

$$\hat{p}_{k\sigma} = i\sqrt{\frac{\hbar ck}{2}}\left(\hat{a}_{k\sigma}{}^{\dagger} - \hat{a}_{-k\sigma}\right)$$

,

And we obtain

$$\left[\hat{a}_{k\sigma}, \hat{a}_{k'\sigma'}{}^{\dagger}\right] = \left[\sqrt{\frac{ck}{2\hbar}}\hat{q}_{k\sigma} + i\sqrt{\frac{1}{2\hbar ck}}\hat{p}_{-k\sigma}, \sqrt{\frac{ck'}{2\hbar}}\hat{q}_{k'\sigma'}{}^{\dagger} - i\sqrt{\frac{1}{2\hbar ck'}}\hat{p}_{-k'\sigma'}{}^{\dagger}\right],$$

$$= \frac{-i}{2\hbar}\left(\sqrt{\frac{k}{k'}}[\hat{q}_{k\sigma}, \hat{p}_{k'\sigma'}] - \sqrt{\frac{k'}{k}}[\hat{p}_{-k\sigma}, \hat{q}_{-k'\sigma'}]\right) = \delta_{\sigma\sigma'}\delta\left(\vec{k} - \vec{k}'\right) \qquad (5.2.13)$$

which now gives

$$\hat{A}(r) = \frac{1}{\sqrt{\varepsilon_o}}\frac{1}{\sqrt{V}}\sum_{k,\sigma}\hat{u}_{k\sigma}e^{-i\vec{k}\vec{r}}\hat{q}_{k\sigma} = \ldots = \sum_{k,\sigma}\sqrt{\frac{\hbar}{2V\varepsilon_0 ck}}\hat{u}_{k\sigma}e^{-i\vec{k}\vec{r}}\hat{a}_{k\sigma} + h.c.,$$

and similarly,

$$\hat{\Pi}_A(r) = \frac{\sqrt{\varepsilon_0}}{\sqrt{V}}\sum_{k,\sigma}\hat{u}_{k\sigma}{}^{*}e^{i\vec{k}\vec{r}}\hat{p}_{k\sigma} = \ldots = i\sum_{k,\sigma}\sqrt{\frac{\varepsilon_0\hbar ck}{2V}}\hat{u}_{k\sigma}e^{-i\vec{k}\vec{r}}\hat{a}_{k\sigma} + h.c..$$

We integrate these operators to get the Hamiltonian with the creation and annihilation operators

$$\hat{q}_{k\sigma} = \sqrt{\frac{\hbar}{2ck}}\left(\hat{a}_{k\sigma} + \hat{a}_{-k\sigma}{}^{\dagger}\right)$$

$$\hat{p}_{k\sigma} = i\sqrt{\frac{\hbar ck}{2}}\left(\hat{a}_{k\sigma}{}^{\dagger} - \hat{a}_{-k\sigma}\right)$$

$$H = \frac{1}{2}\sum_{k,\sigma}\left(\frac{1}{\varepsilon(t)}\hat{p}_{k\sigma}\hat{p}_{k\sigma}{}^{\dagger} + c^2k^2\hat{q}_{k\sigma}\hat{q}_{k\sigma}{}^{\dagger}\right)$$

$$= \frac{1}{2}\sum_{k,\sigma}\left(\frac{1}{\varepsilon(t)}\frac{\hbar ck}{2}\left(\hat{a}_{k\sigma}{}^{\dagger} - \hat{a}_{-k\sigma}\right)\left(\hat{a}_{k\sigma} - \hat{a}_{-k\sigma}{}^{\dagger}\right) + c^2k^2\frac{\hbar}{2ck}\left(\hat{a}_{k\sigma} + \hat{a}_{-k\sigma}{}^{\dagger}\right)\left(\hat{a}_{k\sigma}{}^{\dagger} + \hat{a}_{-k\sigma}\right)\right) \quad (5.2.14)$$

$$= \frac{1}{4}\sum_{k,\sigma}\hbar ck\left(\begin{array}{l}\frac{1}{\varepsilon(t)}\left(\hat{a}_{k\sigma}{}^{\dagger}\hat{a}_{k\sigma} - \hat{a}_{k\sigma}{}^{\dagger}\hat{a}_{-k\sigma}{}^{\dagger} - \hat{a}_{-k\sigma}\hat{a}_{k\sigma} + \hat{a}_{-k\sigma}\hat{a}_{-k\sigma}{}^{\dagger}\right)\\ +\left(\hat{a}_{k\sigma}\hat{a}_{k\sigma}{}^{\dagger} + \hat{a}_{k\sigma}\hat{a}_{-k\sigma} + \hat{a}_{-k\sigma}{}^{\dagger}\hat{a}_{k\sigma}{}^{\dagger} + \hat{a}_{-k\sigma}{}^{\dagger}\hat{a}_{-k\sigma}\right)\end{array}\right)$$

$$= \sum_{k,\sigma}\hbar ck\left(\frac{1}{4}\left(1 + \frac{1}{\varepsilon(t)}\right)\left(\hat{a}_{k\sigma}{}^{\dagger}\hat{a}_{k\sigma} + \hat{a}_{k\sigma}\hat{a}_{k\sigma}{}^{\dagger}\right) + \frac{1}{4}\left(1 - \frac{1}{\varepsilon(t)}\right)\left(\hat{a}_{k\sigma}{}^{\dagger}\hat{a}_{-k\sigma}{}^{\dagger} + \hat{a}_{-k\sigma}\hat{a}_{k\sigma}\right)\right)$$

and the result is the Hamiltonian with creation and annihilation operators of a time-varying medium:

$$H = \sum_{k,\sigma}\hbar ck\left(\frac{1}{2}\left(1 + \frac{1}{\varepsilon(t)}\right)\left(\hat{a}_{k\sigma}{}^{\dagger}\hat{a}_{k\sigma} + \frac{1}{2}\right) + \frac{1}{4}\left(1 - \frac{1}{\varepsilon(t)}\right)\left(\hat{a}_{k\sigma}{}^{\dagger}\hat{a}_{-k\sigma}{}^{\dagger} + \hat{a}_{-k\sigma}\hat{a}_{k\sigma}\right)\right). \quad (5.2.15)$$

It is possible to identify two parts in this Hamiltonian, the single-photon "counting operator" $N_k = a_k^{\dagger}a_k$ and the two-photon-pair creation and annihilation operators. The photon number operator simply defines the energy of each state. On the other hand, the photon-pair creation and annihilation term creates and annihilates pairs of photons, thus constantly changes the number of photons in the system, always operating on pairs of photons with momentum $\pm k$. The action of the two-photon term leads to one of three scenarios: the total number of photons is reduced, increased or remains between some limits. We find that photons with momentum $\hbar k$ related to the band modes of the PTC have an upper bound on the change in the number of photons. On the other hand, in the gap modes the number of photons with $\hbar k$ is exponentially increased or decreased. We show these dynamics in Figure S3, where only the number of photons in the momentum gap is exponentially increased, where the number of photons in the bands never crosses an upper limit, always remaining a small number.

*QED of a PTC*

We use the Hamiltonian of the EM radiation in a time-varying medium we found in the previous section and the vector potential is provided by

$$\hat{A}(r)=\sum_{\vec{k},\sigma}\sqrt{\frac{\hbar}{2\varepsilon_0 Vc|k|n_0}}\mathbf{u}_{k,\sigma}\left(e^{-i\vec{k}\vec{r}}a_{k,\sigma}+e^{i\vec{k}\vec{r}}a_{k,\sigma}^{\dagger}\right). \qquad (5.3.1)$$

For such a system, we can define the eigenmodes of the operator $N_{k,\sigma}=a_{k,\sigma}^{\dagger}a_{k,\sigma}$, which is a photon counting operator. We immediately notice that, if we start with a wavefunction at a specific k value and direction, it can only:

a) Couple to modes with the same polarization $\sigma$
b) Couple to modes with the same $k$ or precisely the opposite wavenumber $-k$.
c) Couple to modes which preserve the Minkowski momentum

$$\vec{M}=\frac{1}{2}\int dr^3\vec{D}\times\vec{B}-\vec{B}\times\vec{D}=\sum_{k.\sigma}\hbar\vec{k}a_{k,\sigma}^{\dagger}a_{k.\sigma} \qquad (5.3.2)$$

The conclusion is that the wavefunction in such a system can be decomposed into modes of the following form

$$|\psi(t)\rangle=\sum_{k\sigma n}|\psi_{k,\sigma,n}(t)\rangle \qquad (5.3.3a)$$

$$|\psi_{k,\sigma,n}\rangle=\sum_{N=n..\infty}b_{k\sigma N}(t)\left|..0..,N_k,(N-n)_{-k},..0..\right\rangle, \qquad (5.3.3b)$$

where $N_k$ is the number of $(k)$-photons, and $(N-n)_{-k}$ is the number of $(-k)$-photons. Of course, the $k$ index includes positive and negative $k$-vectors.
For such a mode, the Minkowski momentum is always conserved and is equal to $\hbar kn$. We can see that from

$$[M,H]=0 \qquad (5.3.4)$$

For these modes, we can reduce the EM Hamiltonian to only its $k$ and $-k$ terms, which results in

$$H_{\pm\vec{k}}(t)=\hbar\frac{c|k|}{n_r}\left[\frac{1}{2}\left(1+\frac{\varepsilon_r}{\varepsilon(t)}\right)\left(a_{k\sigma}^{\dagger}a_{k\sigma}+a_{-k\sigma}^{\dagger}a_{-k\sigma}+1\right)+\frac{1}{2}\left(1-\frac{\varepsilon_r}{\varepsilon(t)}\right)\left(a_{k\sigma}a_{-k\sigma}+a_{k\sigma}^{\dagger}a_{-k\sigma}^{\dagger}\right)\right], \qquad (5.3.5)$$

which is the same as (5.2.15) but accounting for a dielectric refractive index, $n_r$. From now on, we drop the vacuum energy. When this Hamiltonian operates on the state (5.19a), the dynamics is described by

$$H_{\pm\vec{k}}(t)|\psi_{k,\sigma,n}\rangle$$
$$=\sum_{N=n..\infty}\hbar\frac{c|k|}{n_r}\left[\begin{array}{l}\frac{1}{2}b_{k\sigma N}(t)\left(1+\frac{\varepsilon_r}{\varepsilon(t)}\right)(2N-n)|N,N-n\rangle \\ +\frac{1}{2}b_{k\sigma N}(t)\left(1-\frac{\varepsilon_r}{\varepsilon(t)}\right)\left(\begin{array}{l}\sqrt{N(N-n)}|N-1,N-n-1\rangle \\ +\sqrt{(N+1)(N-n+1)}|N+1,N-n+1\rangle\end{array}\right)\end{array}\right]. \qquad (5.3.6)$$

Then, with some algebra, we get the following set (for each N) of equations

$$\dot{b}_{k\sigma nN}(t) = -i\sum_{N=n..\infty}\frac{c|k|}{2n_r}\left[\begin{array}{l}\left(1+\dfrac{\varepsilon_r}{\varepsilon(t)}\right)b_{k\sigma nN}(t)(2N-n)\\ +\left(1-\dfrac{\varepsilon_r}{\varepsilon(t)}\right)\left(\begin{array}{l}b_{k\sigma n,N+1}(t)\sqrt{(N+1)(N-n+1)}\\ +b_{k\sigma n,N-1}(t)\sqrt{N(N-n)}\end{array}\right)\end{array}\right]. \qquad (5.3.7)$$

We note that we can divide the Hamiltonian into two parts, the counting part, for which the photon number with momentum $k$ are found on the diagonal, and the EM interaction term which couples the k and –k photons:

$$\begin{aligned}H(t) &= H_{EM,0} + H_{EM,\text{int}}\\ H_{EM,0}(t) &= \sum_{k>0}\hbar\frac{c|k|}{n_r}\left[\frac{1}{2}\left(1+\frac{\varepsilon_r}{\varepsilon(t)}\right)\left(a^{\dagger}_{k\sigma}a_{k\sigma}+a^{\dagger}_{-k\sigma}a_{-k\sigma}\right)\right] \qquad (5.3.8)\\ H_{EM,\text{int}}(t) &= \sum_{k>0}\hbar\frac{c|k|}{n_r}\left[\frac{1}{2}\left(1-\frac{\varepsilon_r}{\varepsilon(t)}\right)\left(a_{k\sigma}a_{-k\sigma}+a^{\dagger}_{k\sigma}a^{\dagger}_{-k\sigma}\right)\right]\end{aligned}$$

### *1.3 Electron evolution - $H_e$*

The wavefunction of a free-electron accumulates phase over time which is equal to its energy

$$E_e = \gamma mc^2 = \sqrt{m^2c^4+P^2c^2}\ . \quad (5.4.1)$$

In this Cherenkov-type interaction, we assume the electron changes its momentum by the momentum quanta of one photon, which is very small relative to the momentum of the electron

$$\begin{aligned}P' &= P-\hbar k\\ E_e'(k) &= \sqrt{m^2c^4+P'^2c^2},\end{aligned} \qquad (5.4.2)$$

so the energy difference between these two states of the electron is

$$\Delta E_e = E - E_e'(k) = \sqrt{m^2c^4+P^2c^2}\left(1-\sqrt{1+\frac{(\hbar k)^2c^2-2\vec{P}\hbar\vec{k}c^2}{m^2c^4+P^2c^2}}\right)\approx\hbar\vec{k}\cdot\vec{v}\,. \qquad (5.4.3)$$

For states with only these two energies $E_e$ and $E_e'(k)$, the Hamiltonian can be written in a compact form

$$H = \begin{pmatrix}0 & 0\\ 0 & -\hbar\vec{k}\cdot\vec{v}\end{pmatrix}\begin{pmatrix}|P\rangle\\ |P-\hbar k\rangle\end{pmatrix}, \qquad (5.4.4)$$

meaning that the relative phase between the two states of the electron, the state before the emission $|P\rangle$ and the state after the emission $|P-\hbar k\rangle$, is $(\vec{k}\cdot\vec{v})t$.

From energy and momentum considerations and using (5.4.3), we can derive the following law for electron-light interaction in a PTC:

$$E_{e,i}+m\hbar\Omega = E_{e,f}+\hbar\omega_k \rightarrow \vec{k}\cdot\vec{v} = (\omega_k - m\Omega), \qquad (5.4.5)$$

where we assume that the PTC contributes or absorbs energy quanta of $\hbar\Omega$, where $k$ is wavenumber of the emitted photon and $\omega_k$ is the Floquet frequency associated with $k$.

### 1.4 *Interaction between the EM field and the free electron*

The interaction term of a free electron under the influence of an EM field is given by

$$H_{\text{int}} = \frac{e}{m}\hat{P}\cdot\hat{A}\,. \qquad (5.5.1)$$

We can write this term in our case as

$$H_{\text{int}} = \frac{e}{m}\sum_{\vec{k},\sigma}\sqrt{\frac{\hbar}{2\varepsilon_0 Vc|k|n_0}}\hat{P}\cdot\mathbf{u}_{k,\sigma}\left(e^{-i\vec{k}\vec{r}}a_{k,\sigma}+e^{i\vec{k}\vec{r}}a^{\dagger}_{k,\sigma}\right). \qquad (5.52)$$

### 1.5 *Wavefunction evolution in time*

Consider an electron propagating through a medium which has just started changing in time. In this case, our wavefunction is defined by

$$\left|\psi(t)\right\rangle = \sum_{n=0..\infty}\sum_{N=n..\infty} b_{k\sigma nN}(t)\left|P-n\hbar k, N_k, (N-n)_{-k}\right\rangle. \qquad (5.31)$$

The time evolution of this state is

$$i\hbar\frac{d}{dt}\left|\psi(t)\right\rangle = H(t)\left|\psi(t)\right\rangle = \left[H_e + H_{\text{int}} + H_{EM,0}(t) + H_{EM,\text{int}}(t)\right]\left|\psi(t)\right\rangle. \qquad (5.5.3)$$

Then we get

$$\begin{aligned} &i\hbar\frac{d}{dt}\left(\sum_{n=0..\infty}\sum_{N=n..\infty} b_{k\sigma nN}(t)\left|P-n\hbar k, N_k, (N-n)_{-k}\right\rangle\right) \\ &= H(t)\left(\sum_{n=0..\infty}\sum_{N=n..\infty} b_{k\sigma nN}(t)\left|P-n\hbar k, N_k, (N-n)_{-k}\right\rangle\right) \end{aligned}. \qquad (5.5.4)$$

We multiply by each of the states and get the following set of equations:

$$\begin{aligned} &i\hbar\dot{b}_{k\sigma nN}(t) \\ &= b_{k\sigma nN}(t)\left\langle P-n\hbar k, N_k, (N-n)_{-k}\left|E_e + E_{EM,0,k}(t)\right|P-n\hbar k, N_k, (N-n)_{-k}\right\rangle \\ &+b_{k\sigma(n+1)(N+1)}(t)\left\langle P-n\hbar k, N_k, (N-n)_{-k}\left|H_{\text{int}}\right|P-(n+1)\hbar k, (N+1)_k, (N-n)_{-k}\right\rangle \\ &+b_{k\sigma(n-1)(N-1)}(t)\left\langle P-n\hbar k, N_k, (N-n)_{-k}\left|H_{\text{int}}\right|P-(n-1)\hbar k, (N-1)_k, (N-n)_{-k}\right\rangle\Theta(n-1)\Theta(N-1) \\ &+b_{k\sigma(n-1)N}(t)\left\langle P-n\hbar k, N_k, (N-n)_{-k}\left|H_{\text{int}}\right|P-(n-1)\hbar k, N_k, (N-n+1)_{-k}\right\rangle\Theta(n-1) \\ &+b_{k\sigma(n+1)N}(t)\left\langle P-n\hbar k, N_k, (N-n)_{-k}\left|H_{\text{int}}\right|P-(n+1)\hbar k, N_k, (N-n-1)_{-k}\right\rangle\Theta(N-n-1) \\ &+b_{k\sigma n(N+1)}(t)\left\langle P-n\hbar k, N_k, (N-n)_{-k}\left|H_{EM,\text{int}}(t)\right|P-n\hbar k, (N+1)_k, (N+1-n)_{-k}\right\rangle \\ &+b_{k\sigma n(N-1)}(t)\left\langle P-n\hbar k, N_k, (N-n)_{-k}\left|H_{EM,\text{int}}(t)\right|P-n\hbar k, (N-1)_k, (N-1-n)_{-k}\right\rangle\Theta(N-n-1) \end{aligned} \qquad (5.5.5)$$

We substitute this in our Hamiltonian terms, use $\sum_{\sigma}\left\langle P-\hbar k\left|\hat{P}\cdot\mathbf{u}_{k,\sigma}e^{i\vec{k}\vec{r}}\right|P\right\rangle = P\sin(\theta)$ and the approximation $(P-\hbar k)\approx P$, and insert into (5.5.5), to get:

$$
\begin{aligned}
&i\hbar\dot{b}_{k\sigma nN}(t)\\
&=b_{k\sigma nN}(t)\left(-\hbar kv+\hbar\frac{c|k|}{n_r}\left[\frac{1}{2}\left(1+\frac{\varepsilon_r}{\varepsilon(t)}\right)(2N-n)\right]\right)\\
&+b_{k\sigma(n+1)(N+1)}(t)\frac{e}{m}\sqrt{\frac{\hbar}{2\varepsilon_0 Vc|k|n_r}}P\sin(\theta)\sqrt{N+1}\\
&+b_{k\sigma(n-1)(N-1)}(t)\frac{e}{m}\sqrt{\frac{\hbar}{2\varepsilon_0 Vc|k|n_r}}P\sin(\theta)\sqrt{N}\Theta(n-1)\Theta(N-1)\\
&+b_{k\sigma(n-1)N}(t)\frac{e}{m}\sqrt{\frac{\hbar}{2\varepsilon_0 Vc|k|n_r}}P\sin(\theta)\sqrt{N-n+1}\Theta(n-1)\\
&+b_{k\sigma(n+1)N}(t)\frac{e}{m}\sqrt{\frac{\hbar}{2\varepsilon_0 Vc|k|n_r}}P\sin(\theta)\sqrt{N-n}\Theta(N-n-1)\\
&+b_{k\sigma n(N+1)}(t)\hbar\frac{c|k|}{n_r}\left[\frac{1}{2}\left(1-\frac{\varepsilon_r}{\varepsilon(t)}\right)\sqrt{(N+1)(N+1-n)}\right]\\
&+b_{k\sigma n(N-1)}(t)\hbar\frac{c|k|}{n_r}\left[\frac{1}{2}\left(1-\frac{\varepsilon_r}{\varepsilon(t)}\right)\sqrt{(N)(N-n)}\right]\Theta(N-n-1)
\end{aligned}
\qquad (5.5.6)
$$

In our case, we are especially interested in finding the probability of the final state at the reduced momentum (after emitting a single photon of momentum $k$), $P-\hbar k$.

### *1.6* *Simulation of the quantum emission by a free electron below and above the Cherenkov threshold*

For each $k$-vector, we assume a short interaction period such that the emission probability is orders of magnitudes smaller than 1, and calculate the interaction with the time-varying medium using an ODE solver. We calculate the probability by summing over all probabilities of the states with the electron being after the emission of a photon with momentum $\hbar k$, i.e., $|P-\hbar k,0,1\rangle, |P-\hbar k,1,2\rangle, |P-\hbar k,2,3\rangle$, etc. We use the permittivity $\epsilon_r(t)=2+0.1\sin(\Omega t)$, where $\Omega=10^{15}\frac{rad}{s}$. Figure S4A shows the probability of emitting a photon in a time-varying medium when $\beta=0.6<1/n$ at $k_z=3k_g$, where $k_g=\Omega c/2n_{eff}$ (around $60^o$). Figure S4B shows the average probability of emitting a photon $T=50T_c$ for different $k_y$ and $k_z$ values, where $T_c=2\pi/\Omega$ and $\beta$ is equal to 0.95, deep in the superluminal regime. The red curve marks the prediction of the maximum emission from the momentum and energy considerations. This curve corresponds to the lossy emission process, where both the emitted photon and the modulated medium draw energy from the electron.

## 7 Electron velocity change due to the emission of a photon

In this section we calculate the decrease in the electron energy due to photoemission. The relativistic electron energy and photon energies are $E_e = \sqrt{\gamma^2 m_0^2 c^4}$ and $\Delta E = E_{ph} = \hbar\omega$, respectively. We find the dependence of the velocity $\beta$ on a change in the electron's energy:

$$\frac{\partial E_e}{\partial \beta} = \beta(1-\beta^2)^{-\frac{3}{2}} m_0 c^2 \approx \frac{\Delta E}{\Delta \beta}$$

Substituting with the initial electron velocity we obtain

$$\Delta\beta = \frac{(1-\beta_i^2)^{\frac{3}{2}}}{\beta_i m_0 c^2}\Delta E.$$

## 8 Experimental realization

In this section, we suggest an experiment that demonstrates electron light emission in a PTC. To place a relativistic electron in a PTC environment, we suggest to use a UTEM (ultrafast transmission electron microscope [5,6]) system, and illuminate a Lanthanum Boride cathode using an ultrashort UV pulse to create an electron pulse propagating at ~70% of the speed of light. This relativistic electron will be launched into an Aluminum doped Zinc Oxide (AZO) material that can be strongly modulated in time and at very fast time scales [7]. We choose AZO materials because they have an epsilon near zero (ENZ) point at a wavelength of 1500nm. This property immensely enhances nonlinear effects in the medium, by a factor of $1/\sqrt{\epsilon}$. Recent experiments [7] reveal that by transmitting an ultrashort pulse of ~8fs (and rise time of 4fs) through the AZO, the material can cardinally change its electromagnetic properties at few-femtosecond time-scales. We propose to use a train of such pulses to induce a PTC with a change of the refractive index in the near infrared on the order of the refractive index, namely $\frac{\Delta n}{n} \sim 1$.

To realize relativistic collision-free motion of the electron inside the PTC, the electron can pass inside a small vacuum tunnel drawn in this medium, and experience a time-varying EM environment. The tunnel can be smaller than the smallest relevant wavelength, for example, of 200nm diameter, so that the interaction and the emitted light remain practically the same. We show such FDTD simulations in Fig. S5, where the electron passes in a vacuum tunnel 200nm-wide and 600nm-wide carved in a PTC, producing practically the same radiation as an electron passing through a homogenous PTC medium. Alternatively, we also present simulations of the radiation of an electron hovering above a PTC, emitting the same angle-resolved spectrum, but only into the PTC direction. Even when considering only thin samples of AZO fabricated on a substrate, our simulations show that this radiation maintains its main (angle-dependent) features (Fig. S6).

To measure the free-electron interaction with a PTC, we can use a window in the UTEM to do a spectroscopic angle-resolved measurements of the output radiation, using commercial cathodoluminescence techniques [8–10]. Alternatively, we can use electron energy loss spectrometery (EELS) to measure the electrons energy after the interaction, like in [11–15]. A third option is to induce the free-electron radiation in a PTC by stimulated emission, similar to [13,16].In fact, there is no inherent limitation for combining these methods in a single setup.

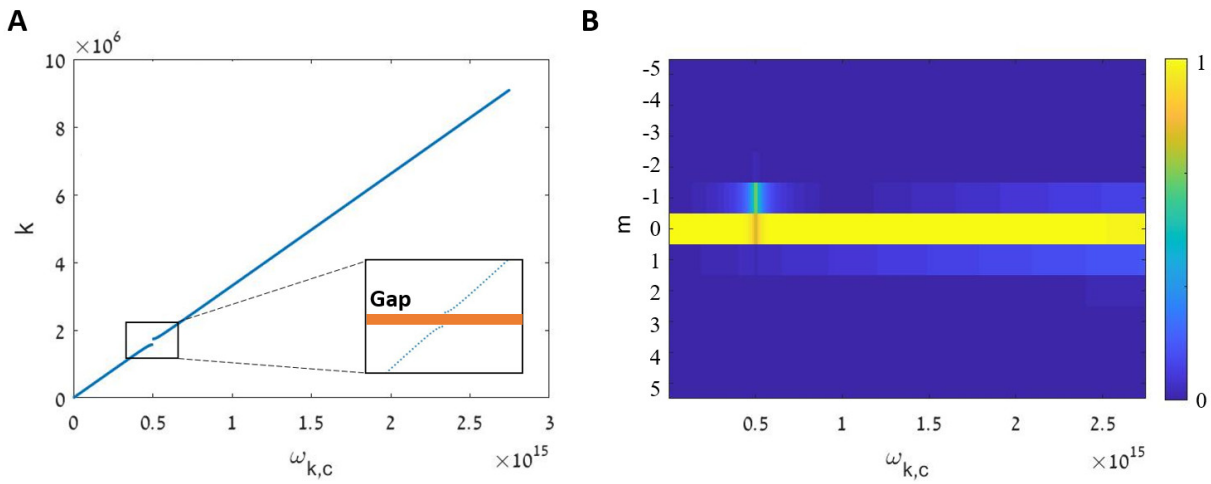


**Figure S1 | Dispersion and mode structure of a sinusoidal PTC.** (A) Dispersion Curve for time-modulated permittivity $\boldsymbol{\epsilon_r = 2 + 0.1\sin(\Omega t)}$. For modulation at $\boldsymbol{\Omega = 10^{15}[\frac{rad}{sec}]}$, a k-gap opens at $\boldsymbol{k = k_g}$ (see lower inset). This dispersion is "unwrapped", meaning that $\omega_{k,c} = \omega_k + l\Omega$, and $\boldsymbol{l}$ counts the $\boldsymbol{\Omega}$ frequency shifts. The inset shows the dispersion curve around the bandgap. (B) Amplitude of the Floquet eigenmode coefficients $\boldsymbol{q_k^m}$, as a function of frequency. At $\boldsymbol{\omega_{k,c} = \frac{\Omega}{2}}$, the Floquet mode has mainly two harmonics, $\boldsymbol{\pm\frac{\Omega}{2}}$. The off-center harmonics ($\boldsymbol{m \neq 0}$) become more dominant for higher frequencies.

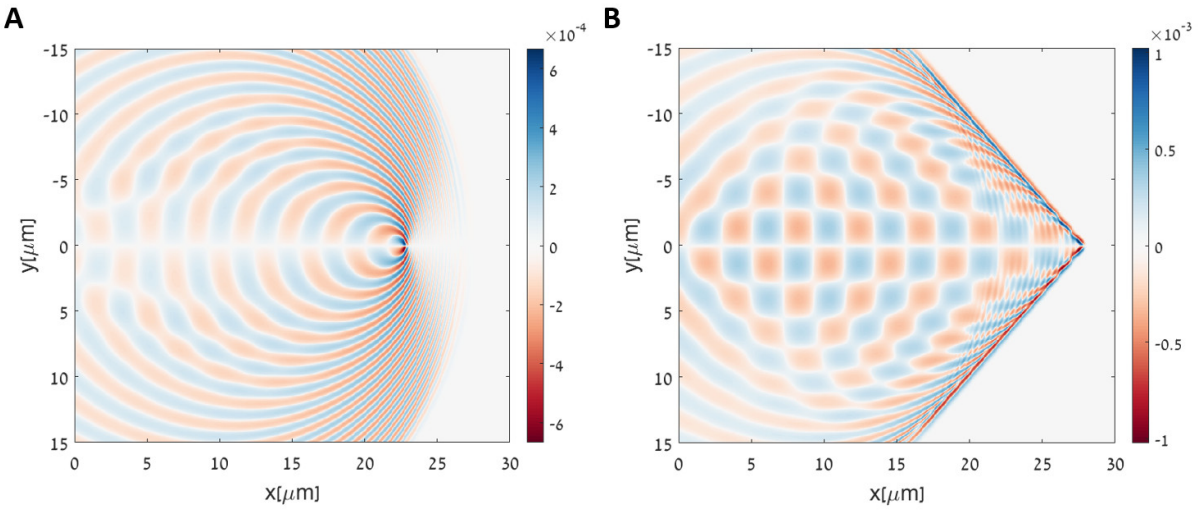


**Figure S2 | Free electron radiation in a PTC, as calculated with FDTD.** (A) The Magnetic field of the radiation by a free electron moving in a PTC below the Cherenkov velocity threshold $\boldsymbol{\beta = 0.6 < \frac{1}{n}}$. (B) Same as (A), where the electron moves above the Cherenkov velocity threshold $\boldsymbol{\beta = 0.9 > \frac{1}{n}}$. Notice the archetypical shockwave structure of the Cherenkov radiation in B superimposed with the multi-directional radiation and the highly enhanced radiation in the momentum gap.

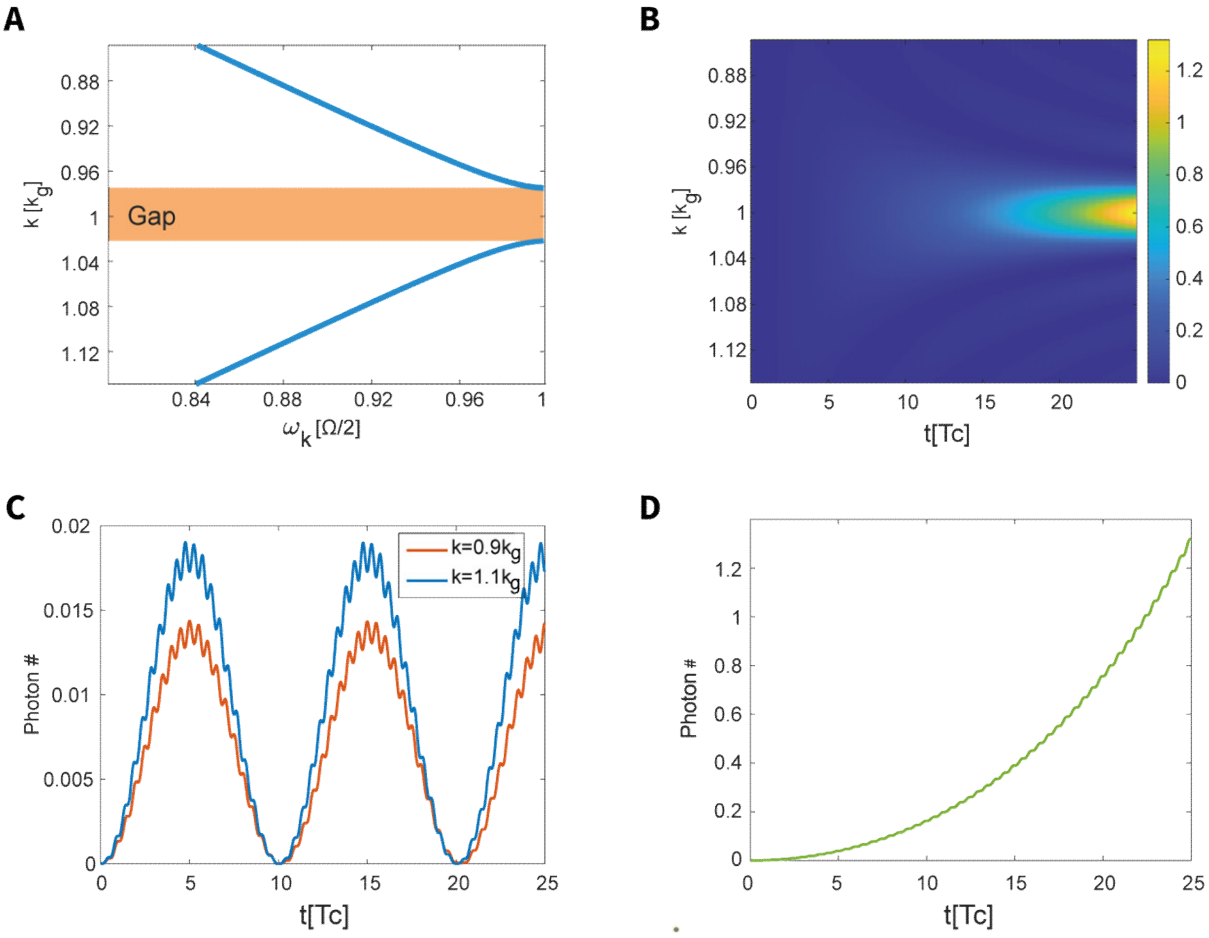


**Figure S3 | Properties of the Hamiltonian descring the EM modes of a PTC.** (A) Band structure of a PTC at the region of the momentum gap. (B) Time evolution of the average photon number for different k values around the momentum gap, where at t=0 the system is in a vacuum state. The number of momentum-gap photons increases exponentially, even if initially there were no bandgap photons in the system. (C), (D) evolution of the average number of photons for $k$ wavenumber 0.9,1 and 1.1 in units of $k_g = \Omega n/2c$. The number of photons in (C) is oscillating and always remaining below some value, but the number of photons in (D) grows exponentially with time, because $k = 1k_g$ is located in the PTC momentum gap.

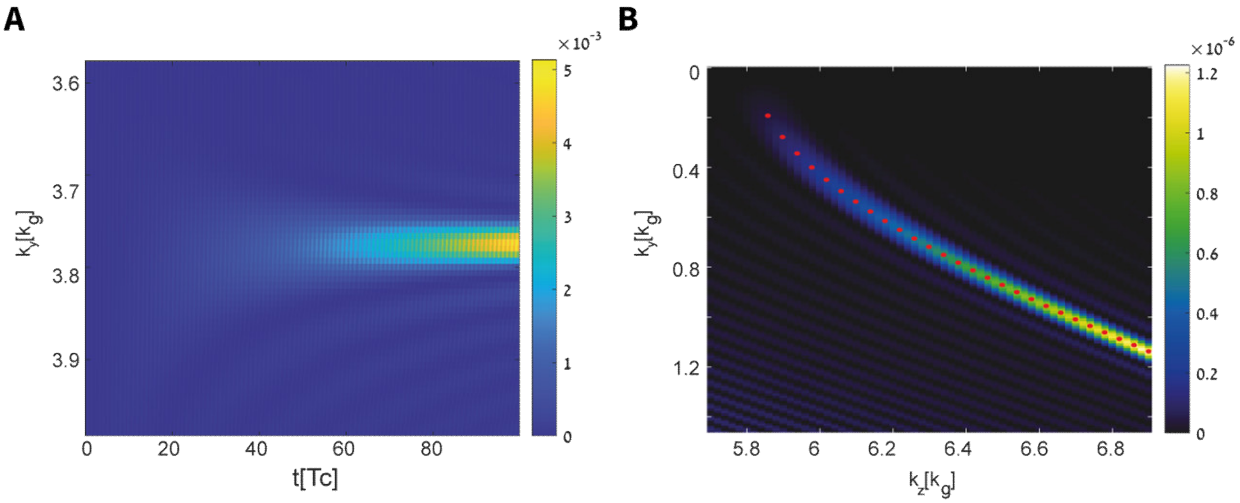


**Figure S4 | Electron emission in a PTC.** (A) Probability of emitting a photon in a PTC as it evolves with time, for $\beta = 0.6 < 1/n$ (subluminal regime) at the angle $k_z = 3k_g$, with $T_c = 2\pi/\Omega$. The $k_y$ for which the growth is the most efficient matches the predicted $k_y$ from Eq. (4) in the main text. (B) Probability of emitting a photon after 50 Floquet cycles T=50$T_c$ for different k values, for $\beta = 0.95 > 1/n$ (superluminal regime). The red curve marks the prediction from the phase-matching condition. This curve corresponds to the lossy emission process, where both the emitted photon and the modulated medium draw energy from the electron.

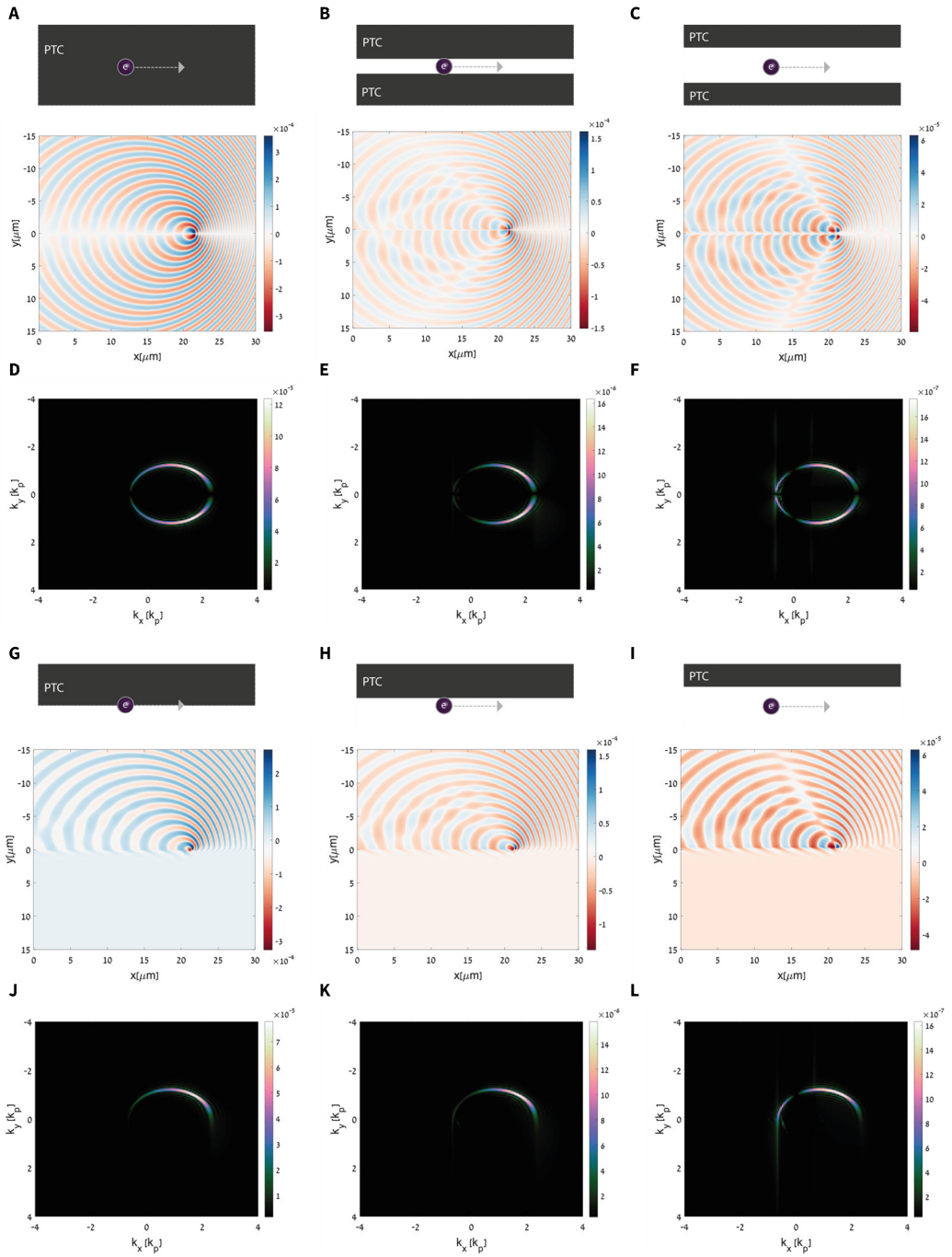


**Figure S5 | Electron radiation in various settings employing PTCs of finite size.** (A-C) Radiation emitted by an electron moving through a hole carved inside a PTC. The hole diameters are 0,200nm and 600nm, respectively (similar to Fig. S2a and Fig. 2e), $\boldsymbol{\epsilon_r = 2}$ and refractive index modulation is of $\mathbf{10^{-3}}$ (r (D-F) Radiation map in k-space of (A-C). (G-I) Radiation emitted by an electron moving near a PTC at a distance of 0,100nm and 300nm from its surface, respectively. (J-L) Radiation map in k-space of (G-I). The angle-resolved radiation features are virtually the same as for an infinite PTC.

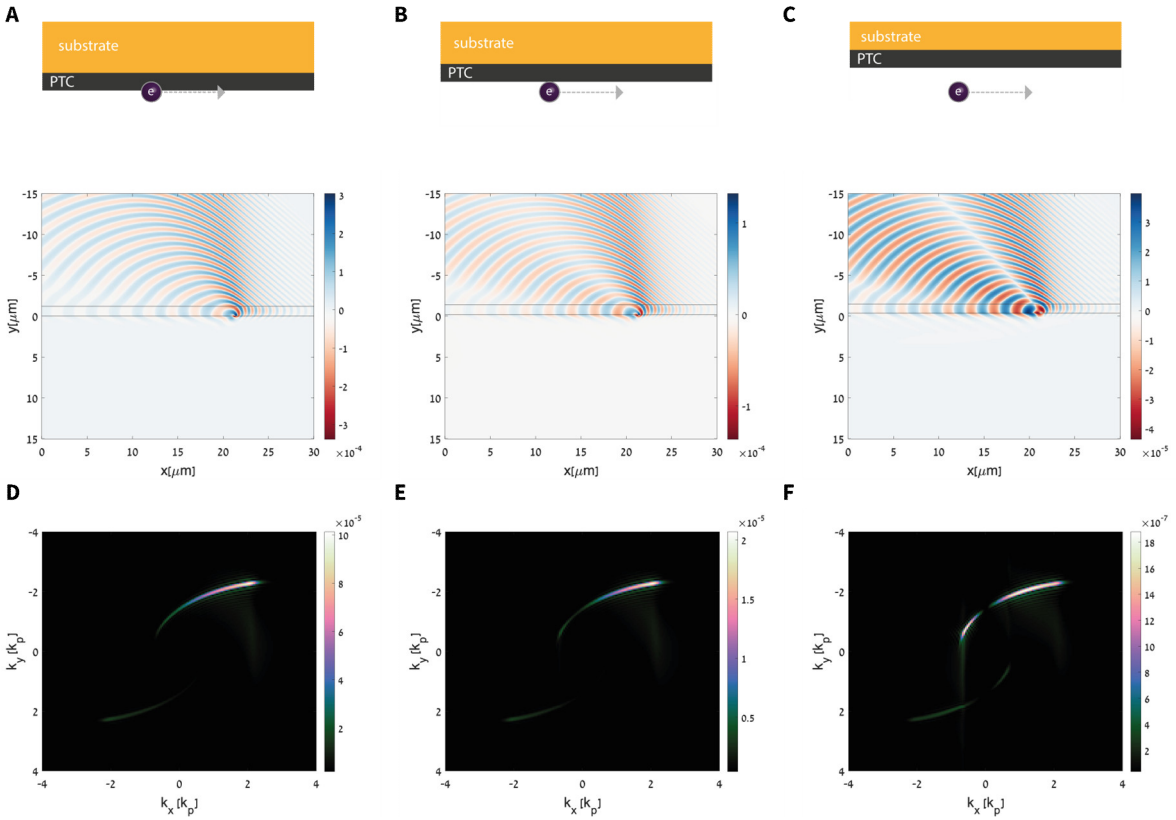


**Figure S6 | Electron radiation using a PTC slab.** (A-C) Radiation emitted by an electron hovering above a PTC slab with 1um width, $\epsilon_r = 2$ and refractive index modulation of $10^{-3}$ at a distance of 0, 100nm and 300nm from the slab, respectively (similar to Fig. S2a and Fig. 2e). The slab is held on a substrate with higher permittivity, $\epsilon_{substr} = 4$. (D-F) Radiation map in k-space of (A-C). The angles of the radiation change due to the transition from low permittivity to high permittivity, but the main features are similar to those in an infinite PTC.

**References**


1. R. E. Slusher, L. W. Hollberg, B. Yurke, J. C. Mertz, and J. F. Valley, "Observation of Squeezed States Generated by Four-Wave Mixing in an Optical Cavity," Phys. Rev. Lett. **55**, 2409–2412 (1985).
2. J. R. Zurita-Sánchez, P. Halevi, and J. C. Cervantes-González, "Reflection and transmission of a wave incident on a slab with a time-periodic dielectric function (t)," Phys. Rev. A - At. Mol. Opt. Phys. **79**, 053821 (2009).
3. H. Minkowski, "The Fundamental Equations for Electromagnetic Processes in Moving Bodies," Math. Klasse 53–111 (1908).
4. E. Lustig, Y. Sharabi, and M. Segev, "Topological aspects of photonic time crystals," Optica **5**, 1390 (2018).
5. B. Barwick, D. J. Flannigan, and A. H. Zewail, "Photon-induced near-field electron microscopy," Nature **462**, 902–906 (2009).
6. F. J. García de Abajo, A. Asenjo-Garcia, and M. Kociak, "Multiphoton Absorption and Emission by Interaction of Swift Electrons with Evanescent Light Fields," Nano Lett. **10**, 1859–1863 (2010).
7. E. Lustig, S. Saha, E. Bordo, C. DeVault, S. N. Chowdhury, Y. Sharabi, A. Boltasseva, O. Cohen, V. M. Shalaev, and M. Segev, "Towards photonic time-crystals: observation of a femtosecond time-boundary in the refractive index," in *Conference on Lasers and Electro-Optics* (Optical Society of America, 2021), p. FF2H.1.
8. E. J. R. Vesseur, R. de Waele, M. Kuttge, and A. Polman, "Direct Observation of Plasmonic Modes in Au Nanowires Using High-Resolution Cathodoluminescence Spectroscopy," Nano Lett. **7**, 2843–2846 (2007).
9. T. Coenen, E. J. R. Vesseur, and A. Polman, "Angle-resolved cathodoluminescence spectroscopy," Appl. Phys. Lett. **99**, 143103 (2011).
10. C. I. Osorio, T. Coenen, B. J. M. Brenny, A. Polman, and A. F. Koenderink, "Angle-Resolved Cathodoluminescence Imaging Polarimetry," ACS Photonics **3**, 147–154 (2016).
11. K. Wang, R. Dahan, M. Shentcis, Y. Kauffmann, A. Ben Hayun, O. Reinhardt, S. Tsesses, and I. Kaminer, "Coherent interaction between free electrons and a photonic cavity," Nature **582**, 50–54 (2020).
12. D. Raphael, G. Alexey, H. Urs, K. Aviv, E. Ori, Y. Peyman, S. Mordechai, A. Ady, E. Gadi, H. Peter, and K. Ido, "Imprinting the quantum statistics of photons on free electrons," Science **373**, 1309–1310 (2021).
13. R. Dahan, S. Nehemia, M. Shentcis, O. Reinhardt, Y. Adiv, X. Shi, O. Be'er, M. H. Lynch, Y. Kurman, K. Wang, and I. Kaminer, "Resonant phase-matching between a light wave and a free-electron wavefunction," Nat. Phys. **16**, 1123–1131 (2020).
14. J. Nelayah, M. Kociak, O. Stéphan, F. J. García de Abajo, M. Tencé, L. Henrard, D. Taverna, I. Pastoriza-Santos, L. M. Liz-Marzán, and C. Colliex, "Mapping surface plasmons on a single metallic nanoparticle," Nat. Phys. **3**, 348–353 (2007).
15. F. J. de Abajo and A. Howie, "Relativistic Electron Energy Loss and Electron-Induced Photon Emission in Inhomogeneous Dielectrics," Phys. Rev. Lett. **80**, 5180–5183 (1998).
16. O. Kfir, H. Lourenço-Martins, G. Storeck, M. Sivis, T. R. Harvey, T. J. Kippenberg, A. Feist, and C. Ropers, "Controlling free electrons with optical whispering-gallery modes," Nature **582**, 46–49 (2020).